

Axio-electric effect

A. Derevianko

Department of Physics, University of Nevada, Reno, Nevada 89557

V. A. Dzuba

*School of Physics, University of New South Wales, Sydney 2052, Australia and
Department of Physics, University of Nevada, Reno, Nevada 89557*

V. V. Flambaum

School of Physics, University of New South Wales, Sydney 2052, Australia

M. Pospelov

*Department of Physics and Astronomy, University of Victoria,
Victoria, British Columbia, V8P IAI, Canada and
Perimeter Institute for Theoretical Physics, Waterloo, Ontario, N2J 2W9, Canada
(Dated: July 13, 2010)*

Using the relativistic Hartree-Fock approximation, we calculate the rates of atomic ionization by absorption of axions of the energies up to 100 keV and for an arbitrary value of the axion mass. We present numerical results for atoms used in the low radioactive background searches of dark matter (*e.g.* Ar, Ge and Xe), as well as the analytical formula which fits numerical calculations for the absorption cross sections and can be applied for other atoms, molecules and condensed matter systems. Using the cross-sections for the axio-electric effect, we derive the counting rates induced by solar axions and set limits on the axion coupling constants.

PACS numbers: 14.70.Pw, 95.35.+d, 32.80.F

I. INTRODUCTION

The idea of dynamical adjustment of the electroweak vacuum that cancels the θ -angle of QCD [1] is perhaps the most natural solution to the strong CP problem. This mechanism inevitably leads to the conclusion about the existence of light pseudoscalar particle in the spectrum, called axion [2]. Breaking of axial $U(1)$ symmetry by QCD anomaly gives a nonperturbative mass to axions with

$$m_a^2 \propto \frac{m_* |\langle \bar{q}q \rangle|}{f_a^2}. \quad (1)$$

Here $m_* = (m_u^{-1} + m_d^{-1})^{-1}$ is the combination of quark masses, $\langle \bar{q}q \rangle$ is the quark condensate and f_a is the axion coupling scale. While original models linked f_a to the weak scale, it was soon realized that it can be in fact arbitrarily large [3], limited only by cosmological and astrophysical considerations (see, *e.g.* [4]).

While the mass of the QCD axion is rigidly linked to its coupling with the topological term $G_{\mu\nu}^a \tilde{G}_{\mu\nu}^a$ via Eq. (1), any axion model allows for additional derivative type couplings to axial currents $J_\mu^A \partial_\mu a / f_a$ of quarks and photons, that obey the shift symmetry of the axion interactions. Over the years a lot of experimental activity has been devoted to detecting axions using interactions of this form. Some methods employ finite cosmological number density of relic axions, while others use the idea of detecting axions that are produced in the solar interior. For a comprehensive review of axion-related phenomenology, see, *e.g.* Refs. [5–7].

A dedicated search for solar axions, such as CAST [8], uses conversion of keV-energy axions into x-ray photons in the magnetic field. Although stringent constraints on the axion coupling constant have been imposed by such searches, only recently did they become competitive with the broad range of astrophysical constraints.

An alternative way of detecting solar axions was proposed in Refs. [9]. The coupling of axions to electrons can lead to the atomic ionization and therefore be searched with high radio-purity materials in the underground experiments. Recent decade has seen a proliferation of such experiments, that source their main scientific motivation in searching for the nuclear recoil from scattering of weakly-interacting massive particles (WIMPs), a putative component of galactic dark matter. Many of these experiments are also able to detect ionization created by solar axions down to a relevant energy scale of a few keV. Some constraints on solar axions were already imposed by the CDMS experiment [11]. This analysis was also extended to the absorption of the super-weakly interacting massive particles (super-WIMPs) that may also plausibly be a dark matter candidate [10]. In case of the pseudoscalar particles, the latter possibility departs, of course, from the mass-coupling relation suggested by (1). To make the distinction clear, we shall designate the solar axions as "massless" or relativistic, and refer to the massive keV-scale axions as super-WIMP possibility. The constraints on super-WIMP axions were improved recently in Ref. [13].

Up until this year, the theory of axio-electric effect was using very simplistic formulae relating the cross sections

of axion absorption to the photo-electric one [12, 14]. Earlier this year, the three of us have updated these calculation for the case of the massive axions using the relativistic Hartree-Fock calculations [15]. In this paper, we calculate the axio-electric effect caused by axions of arbitrary mass, including the relativistic case. Convoluted with the flux of the axions emitted by the solar interior, these results would enable searching/setting limits on the models of light axions that have direct couplings to electrons. Such calculations are especially timely in light of several dark matter experiments have reporting the excess of events over the expected background in the keV region [13] (see also Ref. [16], where the annual modulation of the keV-scale energy deposition is claimed). These results can be generalized to constraints on the emission of other light particles that couple to spin, as *e.g.* in models with additional gauge bosons coupled to the spins of electrons [17].

The main set-up of our calculation is given in the next section. Section 3 presents the results for the axi-electric cross sections. Section 4 contains calculations of the expected signal from the solar axion absorption, and the Appendix provides additional details on atomic calculations.

II. THEORY

The Hamiltonian for the pseudoscalar axion a interacting with electrons can be written in two equivalent ways [14] (see also Appendix)

$$\hat{H}_a = 2 \frac{m_e}{f_a} a \bar{\psi} i \gamma_5 \psi, \quad (2)$$

$$\hat{H}_a = - \frac{\partial_\mu a}{f_a} \bar{\psi} \gamma^\mu \gamma_5 \psi. \quad (3)$$

where energy scale parameter f_a parameterizes the strength of the interaction, m_e is electron mass, a is axion field, ψ is electron Dirac field.

Following our previous work we present the cross section of the atomic ionization by absorbing an axion in a form which contains a dimensionless function of the axion energy $K(\epsilon_a)$:

$$\sigma_a(\epsilon_a) = \left(\frac{\epsilon_0}{f_a} \right)^2 \frac{c}{v} K(\epsilon_a) a_0^2. \quad (4)$$

where ϵ_0 is an energy scale (in our calculations $\epsilon_0=1$ a.u. = 27.21 eV, but it can also be any other energy unit), c is speed of light, v is the axion velocity in the laboratory frame, $a_0 = 0.52918 \times 10^{-8}$ cm is Bohr radius, ϵ_a is axion energy. The function $K(\epsilon_a)$ has no unknown parameters and it is to be found from numerical calculations. It can be presented in a form

$$K(\epsilon_a) = \frac{4\pi}{\alpha^2} \frac{1}{\epsilon_a \epsilon_0^2} \sum_{L,c,\kappa} (2L+1) \langle \kappa | \hat{H}_a | n_c \kappa_c \rangle^2, \quad (5)$$

where c is a state in atomic core, n_c and κ_c are its principal and angular quantum numbers, κ is an angular quantum number for a state in the continuum. Summation over L saturates very rapidly, we cut it at $L_{max} = 3$. We use relativistic Hartree-Fock method to calculate electron wave functions in the core and in the continuum.

The form of the single-electron matrix element depends on the form of the Hamiltonian for the axion-electron interaction (see Appendix for details). The first form (see formula (A9-A11) in the Appendix) is simple. However, it often leads to unstable results. This is due to strong cancellation between the $P_i Q_j$ and $Q_i P_j$ terms in the radial integral. The cancellation is of the order of $1/(Z\alpha)^2$ which means that the formula can be reliably used only for heavy atoms (*e.g.*, Xe).

Second form of the single-electron matrix element (see formulas (A16), (A17) and (A18) in the Appendix) is more complicated. However it is more convenient for the calculations since it gives stable results. In spite of some numerical problems, comparing calculations with two different expressions is a valuable test of the calculations. Two forms of the Hamiltonian must give the same results when exact electron wave functions are used. Since we use the Hartree-Fock wave functions we can have only approximate agreement between results. Therefore, comparing the results is not only a test for the computer code but also a test for the quality of the wave functions used. In our experience the results agree within 10% for the cases when first form gives stable answers. The term “stable” means that variation of the axion energy leads to smooth change in the absorption cross section.

Note that all formulas in the Appendix are for a closed-shell atom. However, this is inessential in our case. We consider axion energies ($\epsilon_a \geq 1$ keV) for which the effect is strongly dominated by inner closed shells while contribution from open valence shells is small and can be neglected. This means that the results can be used for any atom or ion with closed inner shells. They can also be used for molecules and condensed matter systems since inner atomic states depend very little on the environment.

In our present calculations the axion absorption cross section depends on its mass. The only expression which depends on axion mass explicitly is the expression for the axion wave vector

$$k_a = \frac{1}{\hbar c} \sqrt{\epsilon_a^2 - (m_a c^2)^2}. \quad (6)$$

In an extreme case of heavy axion ($m_a c^2 = \epsilon_a$), axion wave vector $k_a = 0$ and only term with $L = 0$ contributes to the summation in (5). This case was considered in our previous work [15].

In present work we consider both these cases. First case gives us a test for the computer code. The results are the same as in our previous calculations [15]. Second case gives new results for axion absorption cross section by atoms. According to Ref. [14] the ratio of the absorption probabilities for these two extreme cases is equal to 2/3

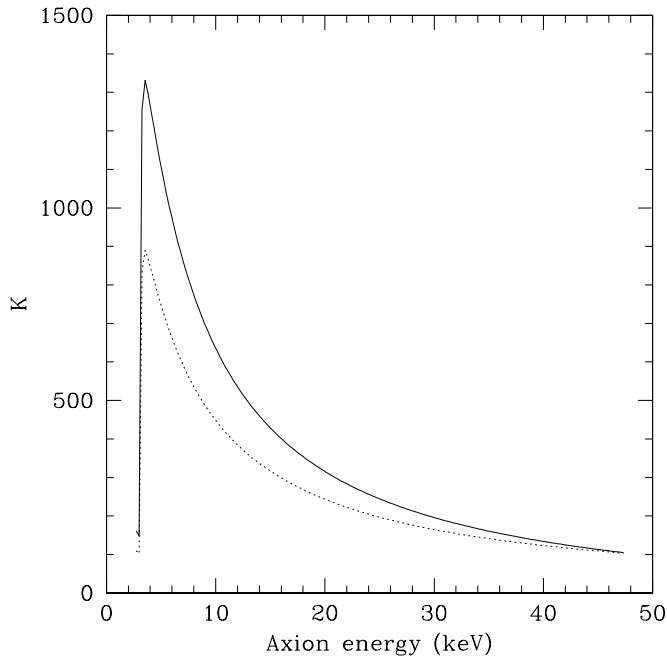


FIG. 1: Dimensionless factor K (see formula (5)) in the ionization cross sections of Ar by axion. Solid line - massive axion ($m_a c^2 = \epsilon_a$), dotted line - massless axion ($m_a = 0$).

in the non-relativistic limit

$$\frac{\sigma_a(m_a = 0)c}{\sigma_a(m_a c^2 = \epsilon_a)v} = \frac{2}{3}. \quad (7)$$

Below we will discuss relativistic corrections to this formula.

III. CALCULATIONS OF THE CROSS SECTIONS

Figures 1,2 and 3 show the results of the relativistic Hartree-Fock calculations for Ar, Ge and Xe of the dimensionless function of the axion energy $K(\epsilon_a)$ which stands in the expression for the cross section of atom ionization by axion (see formula (4)). Many body and relativistic effects beyond the RHF method are ignored and the final electron state in the continuum is calculated in the same potential as initial core state. The accuracy of this approximation is few percents due to dominating contribution from the inner-most core states $1s$, $2s$ and $2p$. For these states the many-body effects are small due to strong nuclear field.

Solid lines on Figures 1, 2 and 3 correspond to the case when all axion energy is due to its mass ($m_a c^2 = \epsilon_a$). This is the same case as was considered in our previous work [15]. Dotted line corresponds to the case of the massless axion ($m_a = 0$). One can see that the ratio of the cross sections is indeed close to $2/3$ at low energies (see formula (7)). However, the ratio becomes larger at

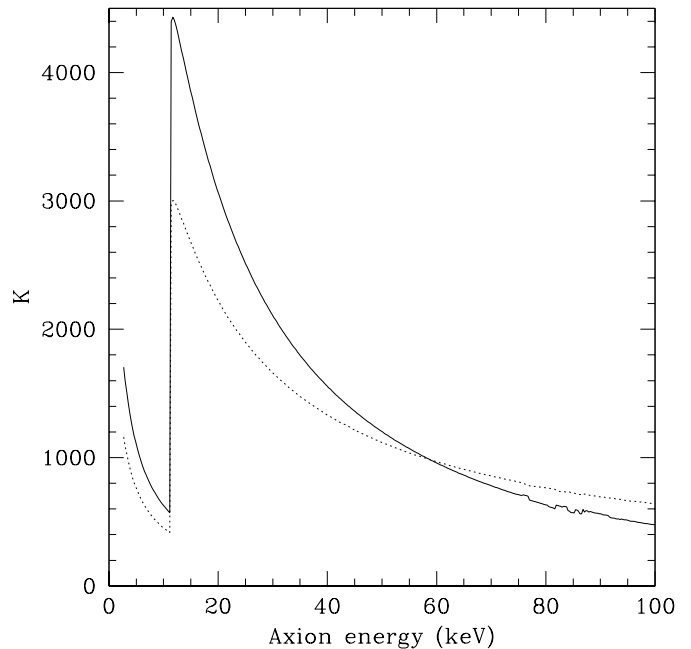


FIG. 2: As on Fig. 1 but for Ge.

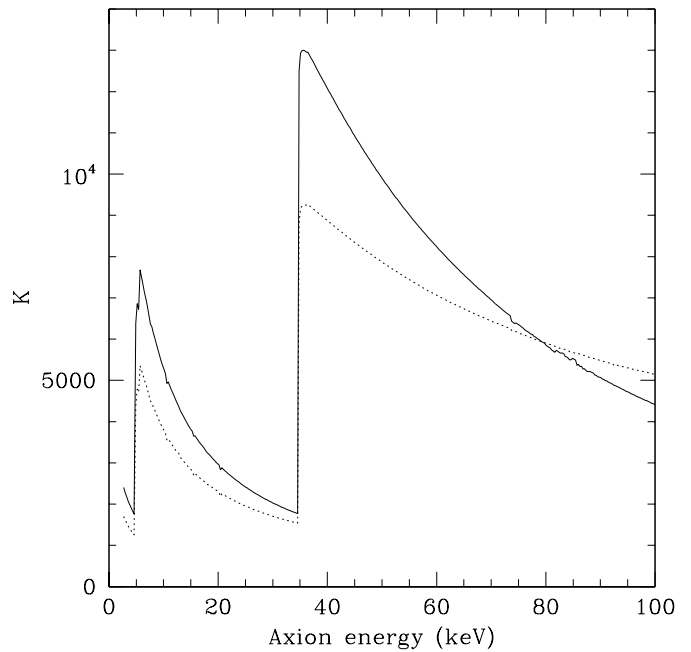


FIG. 3: As on Fig. 1 but for Xe.

high energies. For sufficiently high axion energy the absorption cross section for massless axion becomes larger than those for a massive axion. This is due to the relativistic effects. We found a formula for the ratio of the cross sections which fits very well the numerical calcula-

TABLE I: Hartree-Fock energies of the core states of Na, Ar, Ge, I and Xe (atomic units, 1 a.u.= 27.21 eV).

Atom	Na	Ar	Ge	I	Xe
Z	11	18	32	53	54
1s _{1/2}	-40.54	-119.1	-411.0	-1225.	-1277.
2s _{1/2}	-2.805	-12.41	-53.45	-193.0	-202.4
2p _{1/2}	-1.522	-9.631	-47.33	-180.5	-189.6
2p _{3/2}	-1.514	-9.547	-46.14	-169.5	-177.7
3s _{1/2}	-0.1823	-1.286	-7.409	-40.52	-43.01
3p _{1/2}		-0.5953	-5.324	-35.34	-37.66
3p _{3/2}		-0.5878	-5.157	-33.21	-35.32
3d _{3/2}			-1.616	-24.19	-26.02
3d _{5/2}			-1.591	-23.75	-25.53
4s _{1/2}			-0.5687	-7.759	-8.430
4p _{1/2}			-0.2821	-5.868	-6.452
4p _{3/2}			-0.2730	-5.450	-5.982
4d _{3/2}				-2.341	-2.711
4d _{5/2}				-2.274	-2.633
5s _{1/2}				-0.8762	-1.010
5p _{1/2}				-0.4341	-0.4925
5p _{3/2}				-0.3903	-0.4398

tions. The formula reads

$$R(Z, \epsilon_a) \equiv \frac{\sigma_a(m_a = 0)}{\sigma_a(m_a c^2 = \epsilon_a)} = \frac{2}{3} + 1.5 \times 10^{-5} Z^2 + 1.9 \times 10^{-4} \frac{\epsilon_a + \epsilon_{min}}{\epsilon_0}. \quad (8)$$

Here Z is nuclear charge, ϵ_a is axion energy, ϵ_{min} is the energy of the deepest electron state in the core for which ionization is possible. Note that all states in the core have negative energies, therefore ionization threshold corresponds to the condition $\epsilon_a = -\epsilon_{min}$. Hartree-Fock energies of all core states for Na, Ar, Ge, I and Xe are presented in Table I. The ϵ_0 parameter in (8) is the energy unit. First term on the right-hand side of (8) corresponds to the non-relativistic limit; second term is the relativistic correction due to core electrons; last term is the relativistic correction due to the kinetic energy of the escaping electron.

In our previous work [15] we presented an analytical formula which is an accurate fit of the numerical calculations of the absorption cross section for the massive axion. The formula can be used for wide range of atoms

and axion energies. The formula reads

$$K(m_a c^2 = \epsilon_a) = K_{1s} + K_{2s} + K_{2p}, \quad (9)$$

$$K_{1s} = f_1(Z, \epsilon_a + \epsilon_{1s}) \frac{384\pi\epsilon_{1s}^4}{(\epsilon_0 Z \epsilon_a)^2} \frac{e^{-4\nu_1 \text{arccot} \nu_1}}{1 - e^{-2\pi\nu_1}}, \quad (10)$$

$$K_{2s} = f_2(Z, \epsilon_a + \epsilon_{2s}) \frac{6144\pi\epsilon_2^3}{\epsilon_0 \epsilon_a^2} \left(1 + 3 \frac{\epsilon_2}{\epsilon_a}\right) \times \frac{e^{-4\nu_2 \text{arccot}(\nu_2/2)}}{1 - e^{-2\pi\nu_2}}, \quad (11)$$

$$K_{2p} = f_2(Z, \epsilon_a + \epsilon_{2p}) \frac{12288\pi\epsilon_3^4}{\epsilon_0 \epsilon_a^3} \left(3 + 8 \frac{\epsilon_3}{\epsilon_a}\right) \times \frac{e^{-4\nu_3 \text{arccot}(\nu_3/2)}}{1 - e^{-2\pi\nu_3}}, \quad (12)$$

where α is the fine structure constant, Z is nuclear charge, ϵ_a is axion energy, $\epsilon_2 = |\epsilon_{2s}|$, $\epsilon_3 = |\epsilon_{2p}|$, $\nu_1 = \sqrt{-\epsilon_{1s}/(\epsilon_{1s} + \epsilon_a)}$, $\nu_2 = 2\sqrt{-\epsilon_{2s}/(\epsilon_{2s} + \epsilon_a)}$, $\nu_3 = 2\sqrt{-\epsilon_{2p}/(\epsilon_{2p} + \epsilon_a)}$. Here ϵ_{1s} , ϵ_{2s} and ϵ_{2p} are the Hartree-Fock energies of the core states. Hartree-Fock energies of the 1s, 2s and 2p_{1/2} states of many-electron atoms can be found using extrapolation formulas:

$$\frac{\epsilon_{1s}}{\epsilon_0}(Z) = -\frac{Z^2 - 7.49Z + 43.39}{2}, \quad (13)$$

$$\frac{\epsilon_{2s}}{\epsilon_0}(Z) = -0.000753Z^3 - 0.028306Z^2 - 0.066954Z + 2.359052, \quad (14)$$

$$\frac{\epsilon_{2p}}{\epsilon_0}(Z) = -0.000739Z^3 - 0.027996Z^2 + 0.128526Z + 1.435129. \quad (15)$$

The functions $f_1(Z)$ and $f_2(Z)$ in (10,11,12) are scaling functions:

$$f_1(Z, \epsilon) = (5.368 \times 10^{-7} Z - 1.17 \times 10^{-4})\epsilon/\epsilon_0 - 0.012Z + 1.598 \quad (16)$$

$$f_2(Z, \epsilon) = (-1.33 \times 10^{-6} Z + 1.17 \times 10^{-4})\epsilon/\epsilon_0 - 0.0156Z + 1.15 \quad (17)$$

To find a cross section for massless axion one should take formula (9) and multiply it by the factor $R(Z, \epsilon_a)$ given by (8). Therefore, for the massless axion we also have the results which cover the same range of atoms and energies as in Ref. [15].

IV. SOLAR AXION ABSORPTION SIGNAL

To calculate the rate of the axio-electric effect caused by solar axions, we first address the issue of the total axion flux. Both continuous and line-like emission is possible. Here we take into account the emission of solar axions due to their couplings to nucleons, to photons and to electrons. The easiest case to address is the nuclear case, as it leads to a characteristic $E_a = 14.4$ keV emission due the nuclear transition of the ^{57}Fe nucleus [18].

The solar axion flux was calculated in Ref. [19] (where CAST results were also used to constrain it in combination with coupling of axions to photons). At Earth this flux is given by

$$\Phi_a = 4.5 \times 10^{23} \left(\frac{1 \text{ GeV}}{f_{aN}} \right)^2 \times \text{cm}^{-2} \text{s}^{-1}, \quad (18)$$

where f_{aN} is some effective coupling constant to nucleons that can be related to the coupling of axions to quark spins. The expected counting rates of argon, germanium and xenon experiments are given by

$$R_{\text{Ar}} \simeq 4 \left(\frac{10^6 \text{ GeV}}{(f_a f_{aN})^{1/2}} \right)^4 \text{kg}^{-1} \text{day}^{-1}, \quad (19)$$

$$R_{\text{Ge}} \simeq 18 \left(\frac{10^6 \text{ GeV}}{(f_a f_{aN})^{1/2}} \right)^4 \text{kg}^{-1} \text{day}^{-1}, \quad (20)$$

$$R_{\text{Xe}} \simeq 11 \left(\frac{10^6 \text{ GeV}}{(f_a f_{aN})^{1/2}} \right)^4 \text{kg}^{-1} \text{day}^{-1}, \quad (21)$$

where the following values for the K -factors are used:

$$\begin{aligned} K_{\text{Ar}}(14.4 \text{ keV}) &= 329; \\ K_{\text{Ge}}(14.4 \text{ keV}) &= 2746; \\ K_{\text{Xe}}(14.4 \text{ keV}) &= 2930. \end{aligned}$$

These rates should provide the sensitivity to $(f_a f_{aN})^{1/2}$ in the window between 10^6 and 10^7 GeV. Similar strength constraints were derived in the recent work [20], where a $\sim 3\%$ annual modulation of the axion signal was exploited in conjunction with DAMA results. (Unlike the signal from WIMP dark matter that is expected to have a maximum in June, the solar axion signal is minimized in early July.) We leave it to the experimental collaborations to determine the exact upper limits on solar axions ensuing from their results.

If the coupling to photons is not zero, $F_{\mu\nu} \tilde{F}_{\mu\nu} a / (4f_{a\gamma})$, then we can calculate the counting rate, using the axion flux provided in Ref. [8]:

$$\frac{d\Phi_a}{d\epsilon_a} = 6.02 \times 10^{30} \left(\frac{1 \text{ GeV}}{f_{a\gamma}} \right)^2 \epsilon_a^{2.481} e^{-\frac{\epsilon_a}{1.205}} \quad (22)$$

$\times \text{cm}^{-2} \text{s}^{-1} \text{keV}^{-1}.$

Counting rate for the axio-electric effect is given by the product of the calculated absorption cross section and the flux (22). For $(f_a f_{a\gamma})^{1/2}$ normalized on 10^8 GeV, we get the counting rates plotted in Figure 4. Integration over axion energy leads to the following total counting rates

$$R_{\text{Ar}} \simeq 5.0 \left(\frac{10^8 \text{ GeV}}{(f_a f_{a\gamma})^{1/2}} \right)^4 \text{kg}^{-1} \text{day}^{-1}, \quad (23)$$

$$R_{\text{Ge}} \simeq 5.2 \left(\frac{10^8 \text{ GeV}}{(f_a f_{a\gamma})^{1/2}} \right)^4 \text{kg}^{-1} \text{day}^{-1}, \quad (24)$$

$$R_{\text{Xe}} \simeq 8.2 \left(\frac{10^8 \text{ GeV}}{(f_a f_{a\gamma})^{1/2}} \right)^4 \text{kg}^{-1} \text{day}^{-1}. \quad (25)$$

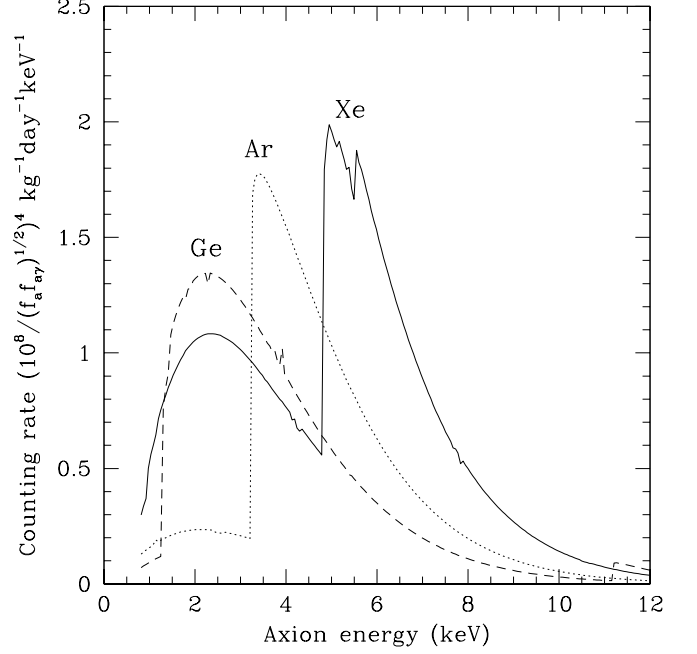


FIG. 4: Counting rate for the axio-electric effect for Ar, Ge and Xe as a function of axion energy.

Comparing this to the counting rate of the CDMS experiment [11], one can see that the equivalent of $(f_a f_{a\gamma})^{1/2} \sim 10^8$ GeV are being probed, as the counting rates in the window from 1.5 to 4 keV reach $O(1 \text{ kg}^{-1} \text{day}^{-1} \text{keV}^{-1})$. Similar sensitivity is achieved in the CoGent experiment [13].

Finally, the axion flux can be created by the emission of the axions due to the same interaction that leads to atomic ionization. In this case, however, the production cross section is down by additional factor of E_a^2/m_e^2 [14], and the sensitivity to f_a in this case does not exceed 10^6 GeV.

V. CONCLUSIONS

QCD axions represent one of the most well-motivated extensions of the Standard Model. Their light mass and small couplings allow them to be produced in the Solar interior and escape reaching the Earth. With the proliferation of the low-background searches of dark matter, one should also conduct searches of solar axions. In this paper we have calculated the cross sections relevant for these searches, improving upon the simple scaling relations that tie the axio-electric and photo-electric effects.

Last two years has brought a significant progress in sensitivity to any ionizing effects in Germanium in the window from 1 to 10 keV [11, 13]. Currently, the CoGent experiment has very low backgrounds in the window from 2 to 4 keV, where the solar axion signal is expected to peak. With acquiring more statistics, the sensitivity

to the solar axions in this experiment is poised to grow. We also remark at this point that the excess of events recorded by CoGent below 1 keV does not fit the expected shape of the spectrum from solar axions. Future progress in searching for solar axions may also come from the large scale detectors with self-shielding capabilities.

Acknowledgments

This work was supported in part by the Australian Research Council, and the NSERC of Canada. Research at Perimeter Institute is also supported in part by NSERC and by the Province of Ontario through MEDT.

Appendix A: Derivation of cross-section for the axio-electric effect

There are two equivalent expressions for the Lagrangian describing coupling of pseudoscalar axions of mass m_a to electrons

$$H_a = 2 \frac{m_e}{f_a} a \bar{\psi} i \gamma_5 \psi, \quad (A1)$$

$$H'_a = -\frac{1}{f_a} (\partial_\mu a) \bar{\psi} \gamma^\mu \gamma_5 \psi. \quad (A2)$$

Here ψ is the electronic wave function and f_a is a coupling constant. The axion field a may be represented as

$$a = N e^{i(\mathbf{k} \cdot \mathbf{r} - \omega t)} = N e^{-ik_\lambda x^\lambda},$$

with the dispersion relation

$$\hbar\omega = k_0 = \sqrt{(mc^2)^2 + (\hbar c |\mathbf{k}|)^2},$$

and N being the normalization constant.

We will treat the axio-ionization in the independent-particle approximation (IPA) for atom. In the IPA, the atomic many-body wave function is represented by a single Slater determinant built from single-particle atomic orbitals. Then, as a result of the axio-ionization, an atomic electron in the initial single-particle orbital will be ejected into a continuum state. The standard prescription for evaluating cross-sections due to H_a and H'_a requires computing matrix elements of transition operators,

$$T_a = -e^{i\mathbf{k} \cdot \mathbf{r}} i \gamma_0 \gamma_5, \quad (A3)$$

$$T'_a = \frac{1}{2} e^{i\mathbf{k} \cdot \mathbf{r}} (i k_\mu) \gamma_0 \gamma^\mu \gamma_5. \quad (A4)$$

In the last formula $\gamma_0 k_\mu \gamma^\mu \gamma_5 = \gamma_5 k_0 - \mathbf{k} \cdot \boldsymbol{\sigma}$. Formal equivalence of matrix elements from pseudoscalar and axial-vector forms of the interactions was demonstrated in Ref. [14] with the use of the single-electron Dirac equation with arbitrary potential.

Since atoms are spherically-symmetric, we employ the standard machinery of the angular momentum algebra [22] and use the partial wave expansion for evaluating cross-sections. In particular, at large values of electronic coordinate the continuum orbital has to go over to a sum of an incoming spherical and plane waves [21]. Scattering wave function satisfying this boundary condition may be decomposed in partial waves

$$w_{\mathbf{p}\lambda} = N_p \sum_{\kappa m} (\Omega_{\kappa m}^\dagger(\hat{\mathbf{p}}) \chi_\lambda) i^{l-1} e^{-i\delta_\kappa} w_{\kappa m}(\mathbf{r}). \quad (A5)$$

Here $\Omega_{\kappa m}$ is a spherical spinor, χ_σ is a two-component spinor describing spin-polarization of the photoelectron, the relativistic angular quantum number $\kappa = (l-j)(2j+1)$ is expressed in terms of the total j and orbital l angular momenta, and δ_κ is a scattering phase shift. For box-normalized solutions (V is the volume of the box, p and E are the momentum and the energy of the electron, and α_{fs} is the fine-structure constant)

$$N_p = \left(\frac{(2\pi)^3}{\alpha_{fs} E p V} \right)^{1/2}.$$

Wave function $w_{\kappa m}(\mathbf{r})$ may be expressed in terms of the large (S_κ) and small (T_κ) components satisfying the radial Dirac equations

$$w_{\kappa m}(\mathbf{r}) = \frac{1}{r} \begin{pmatrix} i S_\kappa(r) \Omega_{\kappa m}(\hat{\mathbf{r}}) \\ T_\kappa(r) \Omega_{-\kappa m}(\hat{\mathbf{r}}) \end{pmatrix}. \quad (A6)$$

For bound-state orbitals, the parameterization reads

$$|n_b \kappa_b m_b\rangle = \frac{1}{r} \begin{pmatrix} i P_{n\kappa}(r) \Omega_{\kappa m}(\hat{\mathbf{r}}) \\ Q_{n\kappa}(r) \Omega_{-\kappa m}(\hat{\mathbf{r}}) \end{pmatrix}. \quad (A7)$$

Axio-ionization cross-sections are proportional to the square of transition amplitudes. Averaging it over all possible spin polarizations λ , magnetic quantum numbers m_b and m and integrating over the directions of the ejected electron momentum, we find $\sum_{\lambda \kappa m m_b \kappa_b} \int |\langle w_{\mathbf{p}\lambda} | T_a | n_b \kappa_b m_b \rangle|^2 d\Omega_p = N_p^2 \sum_{\kappa m m_b} |\langle w_{\kappa m} | T_a | n_b \kappa_b m_b \rangle|^2$. The same result holds for the averaged square of T'_a operator.

The involved matrix element $\langle w_{\kappa m} | T_a | n_b \kappa_b m_b \rangle$ is between the electronic states of definite angular momenta and parity. For simplifying summations over magnetic quantum numbers, we expand the transition operators into irreducible tensor operators (ITO) and then apply the Wigner-Eckart theorem.

We start with the simpler case of operator (A3). We employ the conventional expansion

$$e^{i\mathbf{k} \cdot \mathbf{r}} = \sum_{LM} [L] i^L j_L(kr) C_{LM}^*(\hat{\mathbf{k}}) C_{LM}(\hat{\mathbf{r}}),$$

where C_{LM} are the normalized spherical harmonics [22] and $[L] = 2L + 1$. Then we reexpress the transition operator as

are ITOs of rank L . A matrix element evaluated between two atomic orbitals reads

$$T_a = -e^{i\mathbf{k}\cdot\mathbf{r}} i\gamma_0\gamma_5 = \sum_{LM} i^L [L] C_{LM}^*(\hat{k}) \tau_{LM}(\mathbf{r}). \quad (\text{A8})$$

Here the operators

$$\tau_{LM}(\mathbf{r}) = -i\gamma_0\gamma_5 j_L(kr) C_{LM}(\hat{r})$$

$$(\tau_{LM})_{ij} = -\langle \kappa_i m_i | C_{LM} | -\kappa_j m_j \rangle \left(\int_0^\infty j_L(kr) [P_{n_i\kappa_i}(r) Q_{n_j\kappa_j}(r) + Q_{n_i\kappa_i}(r) P_{n_j\kappa_j}(r)] dr \right)$$

The selection rules for matrix elements of the C-tensor require that $|j_i - j_j| \leq L \leq j_i + j_j$ and $L + l_i + l_j = \text{odd}$. For example, for $L = 0$ the multipolar operator is pseudoscalar: the τ_{00} operator drives $s_{1/2} \rightarrow p_{1/2}$ transitions. Reduced matrix element

$$\langle n_i \kappa_i || \tau_L || n_j \kappa_j \rangle = -\langle \kappa_i || C_L || -\kappa_j \rangle \left(\int_0^\infty j_L(kr) [P_{n_i\kappa_i}(r) Q_{n_j\kappa_j}(r) + Q_{n_i\kappa_i}(r) P_{n_j\kappa_j}(r)] dr \right). \quad (\text{A9})$$

To evaluate the cross-section we fix the coordinate system in such a way that the axion propagates along the z -axis. Then in Eq.(A8),

$$C_{LM}^*(\hat{k}) = \delta_{M0} \text{ and } T_a = \sum_L i^L [L] \tau_{LM=0}(\mathbf{r}). \quad (\text{A10})$$

Further

$$\sum_{\lambda\kappa m} \sum_{n_b\kappa_b m_b} \int |\langle w_{\mathbf{p}\lambda} | T_a | n_b\kappa_b m_b \rangle|^2 d\Omega_p = N_p^2 \sum_{n_b\kappa_b\kappa_L} (2L+1) (\langle \kappa || \tau_L || n_b\kappa_b \rangle)^2.$$

Finally,

$$\sigma = \frac{c}{v} \frac{4\pi}{\alpha_{fs}^2} \frac{1}{f_a^2} \frac{1}{\varepsilon_a} \times \sum_{n_b\kappa_b\kappa_L} (2L+1) (\langle \kappa || \tau_L || n_b\kappa_b \rangle)^2. \quad (\text{A11})$$

Derivation of the axio-ionization cross-section for the alternative form of the coupling H'_a is more complicated. We start from the multipole expansion of the T'_a operator,

$$T'_a = \frac{1}{2} i (\gamma_5 k_0 - \mathbf{k} \cdot \boldsymbol{\sigma}) e^{i\mathbf{k}\cdot\mathbf{r}} = \sum_{LM} i^L [L] C_{LM}^*(\hat{k}) \tau'_{LM}(\mathbf{r}). \quad (\text{A12})$$

Because the angular dependence of this expansion is the same as in Eq.(A8), the expression for the cross-section remains the same as in the H_a case, Eq.(A11), with the substitution $\tau_L \rightarrow \tau'_L$.

The multipolar tensors τ'_{LM} may be derived by inverting the expansion (A12)

$$\begin{aligned} \tau'_{LM}(\mathbf{r}) &= \frac{i^{-L}}{4\pi} \int d\Omega_k C_{LM}(\hat{k}) \frac{1}{2} i (\gamma_5 k_0 - \mathbf{k} \cdot \boldsymbol{\sigma}) e^{i\mathbf{k}\cdot\mathbf{r}} = \\ &= \sum_{L'M'} i^{L'-L} [L'] j_{L'}(kr) C_{L'M'}(\hat{r}) \frac{1}{4\pi} \int d\Omega_k C_{LM}(\hat{k}) \frac{1}{2} i (\gamma_5 k_0 - \mathbf{k} \cdot \boldsymbol{\sigma}) C_{L'M'}^*(\hat{k}). \end{aligned}$$

The two contributions to the integral are

$$\frac{1}{4\pi} \int d\Omega_k C_{LM}(\hat{k}) C_{L'M'}^*(\hat{k}) \frac{1}{2} i (\gamma_5 k_0) = \frac{1}{[L]} \frac{1}{2} i (\gamma_5 k_0) \delta_{LL'} \delta_{MM'} \quad (\text{A13})$$

and

$$\frac{1}{4\pi} \int d\Omega_k C_{LM}(\hat{k}) C_{L'M'}^*(\hat{k}) \frac{1}{2} i (-\mathbf{k} \cdot \boldsymbol{\sigma}) = -\frac{1}{2} |\mathbf{k}| i (\boldsymbol{\sigma} \cdot \mathbf{a}_{L'M';LM}), \quad (\text{A14})$$

where the components of a vector object $\mathbf{a}_{L'M';LM}$

$$(\mathbf{a}_{L'M';LM})_\lambda = \frac{1}{4\pi} \int d\Omega_k C_{L'M'}^* (\hat{k}) \hat{k}_\lambda C_{LM} (\hat{k}) = \frac{1}{\sqrt{[L][L']}} \langle L'M' | C_{1\lambda} | LM \rangle. \quad (\text{A15})$$

The resulting expression reads

$$\tau'_{LM}(\mathbf{r}) = \tau t'_{LM}(\mathbf{r}) + \tau s'_{LM}(\mathbf{r}) = j_L(kr) C_{LM'}(\hat{r}) \frac{1}{2} i(\gamma_5 k_0) - \frac{1}{2} |\mathbf{k}| \sum_{L'M'} i^{L'-L+1} [L'] j_{L'}(kr) C_{L'M'}(\hat{r}) (\boldsymbol{\sigma} \cdot \mathbf{a}_{L'M';LM}),$$

where we split the operator into the time- and space-like contributions. Below we tabulate reduced matrix elements of the τ'_{LM} ITO

$$\langle n_i \kappa_i | \tau'_L | n_j \kappa_j \rangle = \langle n_i \kappa_i | \tau t'_L | n_j \kappa_j \rangle + \langle n_i \kappa_i | \tau s'_L | n_j \kappa_j \rangle, \quad (\text{A16})$$

$$\langle n_i \kappa_i | \tau t'_L | n_j \kappa_j \rangle = \frac{1}{2} k_0 \langle \kappa_i | C_L | -\kappa_j \rangle \left(\int_0^\infty j_L(kr) [P_{n_i \kappa_i}(r) Q_{n_j \kappa_j}(r) - Q_{n_i \kappa_i}(r) P_{n_j \kappa_j}(r)] dr \right), \quad (\text{A17})$$

$$\begin{aligned} \langle n_i \kappa_i | \tau s'_L | n_j \kappa_j \rangle = & -\frac{1}{2} |\mathbf{k}| \sum_{L'=L-1, L+1; L' \geq 0} i^{L'-L+1} \langle \kappa_i | A_{L'} | \kappa_j \rangle [L'] \times \\ & \left(\int_0^\infty j_{L'}(kr) [P_{n_i \kappa_i}(r) P_{n_j \kappa_j}(r) + Q_{n_i \kappa_i}(r) Q_{n_j \kappa_j}(r)] dr \right), \end{aligned} \quad (\text{A18})$$

with

$$\begin{aligned} \langle \kappa' | A_{L'} | \kappa \rangle = & \langle \kappa' | \sum_{M'} C_{L'M'}(\hat{r}) (\boldsymbol{\sigma} \cdot \mathbf{a}_{L'M';LM}) | \kappa \rangle = \\ & \frac{[j, j', l, l']^{1/2}}{[L, L']^{1/2}} \sqrt{6} (-1)^{j'+j} (-1)^{L'+l} \begin{pmatrix} l' & L' & l \\ 0 & 0 & 0 \end{pmatrix} \begin{pmatrix} L' & 1 & L \\ 0 & 0 & 0 \end{pmatrix} \begin{Bmatrix} 1 & L' & L \\ 1/2 & l' & j' \\ 1/2 & l & j \end{Bmatrix}. \end{aligned}$$

Here the notation $[J_1, \dots, J_n] = (2J_1 + 1) \dots (2J_n + 1)$. The two-row quantities are the 3j-symbols and the 3x3 matrix in the curly brackets is the 9j-symbol. Notice that the phase $i^{L'-L+1}$ entering Eq.(A18) is either +1 or -1, i.e., the entire expression is real. Selection rules for both time- and space-like contributions are the same as in the case of the τ_{LM} multipoles: $|j_i - j_j| \leq L \leq j_i + j_j$ and $L + l_i + l_j = \text{odd}$.

To summarize, the cross-section for axio-ionization is given by Eq. (A11), with reduced matrix elements given by Eqs. (A9) and (A16). Notice that the derived expressions remain valid for arbitrary large values of parameter kr , i.e., even when the usual dipole approximation ($e^{ikr} \approx 1$) breaks down.

-
- | | |
|--|---|
| <p>[1] R. D. Peccei and H. R. Quinn, Phys. Rev. Lett. 38, 1440 (1977).</p> <p>[2] S. Weinberg, Phys. Rev. Lett. 40, 223 (1978); F. Wilczek, Phys. Rev. Lett. 40, 279 (1978).</p> <p>[3] J. E. Kim, Phys. Rev. Lett. 43, 103 (1979); M. A. Shifman, A. I. Vainshtein and V. I. Zakharov, Nucl. Phys. B 166, 493 (1980); M. Dine, W. Fischler and M. Srednicki, Phys. Lett. B 104, 199 (1981); A. R. Zhitnitsky, Sov. J. Nucl. Phys. 31, 260 (1980) [Yad. Fiz. 31, 497 (1980)].</p> <p>[4] R. D. Peccei, J. Korean Phys. Soc. 29, S199 (1996) [arXiv:hep-ph/9606475].</p> <p>[5] M. S. Turner, Phys. Rept. 197, 67 (1990).</p> <p>[6] R. Bradley <i>et al.</i>, Rev. Mod. Phys. 75, 777 (2003).</p> | <p>[7] G. G. Raffelt, Ann. Rev. Nucl. Part. Sci. 49, 163 (1999) [arXiv:hep-ph/9903472].</p> <p>[8] S. Andriamonje <i>et al.</i> [CAST Collaboration], JCAP 0704, 010 (2007) [arXiv:hep-ex/0702006].</p> <p>[9] F. T. Avignone <i>et al.</i>, Phys. Rev. D 35, 2752 (1987).</p> <p>[10] R. Bernabei <i>et al.</i>, Int. J. Mod. Phys. A 21, 1445 (2006) [arXiv:astro-ph/0511262].</p> <p>[11] Z. Ahmed <i>et al.</i> [CDMS Collaboration], Phys. Rev. Lett. 103, 141802 (2009) [arXiv:0902.4693 [hep-ex]].</p> <p>[12] S. Dimopoulos, G. D. Starkman and B. W. Lynn, Phys. Lett. B 168, 145 (1986).</p> <p>[13] C. E. Aalseth <i>et al.</i> [CoGeNT collaboration], arXiv:1002.4703 [astro-ph.CO].</p> |
|--|---|

- [14] M. Pospelov, A. Ritz, M. Voloshin, Phys. Rev. D **78**, 115012 (2008).
- [15] V. A. Dzuba, V. V. Flambaum, and M. Pospelov, Phys. Rev. D **81**, 103520 (2010).
- [16] R. Bernabei *et al.* [DAMA Collaboration], Eur. Phys. J. C **56**, 333 (2008) [arXiv:0804.2741 [astro-ph]].
- [17] B. A. Dobrescu, Phys. Rev. Lett. **94**, 151802 (2005) [arXiv:hep-ph/0411004].
- [18] W. C. Haxton and K. Y. Lee, Phys. Rev. Lett. **66**, 2557 (1991).
- [19] S. Andriamonje *et al.* [CAST Collaboration], JCAP **0912**, 002 (2009) [arXiv:0906.4488 [hep-ex]].
- [20] F. T. Avignone, R. J. Creswick and S. Nussinov, Phys. Lett. B **681**, 122 (2009).
- [21] John R. Taylor, *Scattering Theory : The Quantum Theory of Non-Relativistic Collisions*, R.E. Krieger Pub. Co, Malabar, Fla. (1983).
- [22] D. A. Varshalovich, A. N. Moskalev, and V. K. Khersonskii, *Quantum Theory of Angular Momentum*, World Scientific, Singapore (1988).